Departures from the principle of superposition in silicon solar cells

S. J. Robinson, A. G. Aberle,[a] and M. A. Green
Centre for Photovoltaic Devices and Systems, University of New South Wales, Sydney 2052, Australia

(Received 11 March 1994; accepted for publication 15 August 1994)

The principle of superposition forms the theoretical basis on which the comparison of illuminated and dark current-voltage (I-V) characteristics of solar cells depends. Two cases predicted from computer simulations where the superposition principle does *not* apply in silicon p-n junction solar cells are reported. These predictions are confirmed experimentally with measurements taken on existing high-efficiency devices, and cannot be accurately described by previous explanations for departures from this principle. The first case, which is the more important in terms of operation under 1 sun illumination, occurs in cells where recombination via defect levels (Shockley–Read–Hall recombination) with unequal electron and hole capture rates dominates the I-V characteristics. The second case is evident at small forward voltages in almost all silicon solar cells. It is shown that the former is due to a saturation in the recombination rate, while the latter is the result of a bias-dependent modification of the carrier concentrations across the p-n junction depletion region which is different under illumination from that in the dark.

I. INTRODUCTION

Analysis of solar-cell I-V characteristics is often performed using the so-called "shifting approximation,"[1] where the illuminated I-V curve (which, in this work, we assume lies in the fourth quadrant), shifted by the short-circuit current J_{sc}, is assumed to very closely approximate the dark I-V curve. Algebraically,

$$J_L(V)-J_{sc}=J_D(V), \tag{1}$$

where J_L and J_D are the current densities under illumination and in the dark, respectively. (In this formalism the short-circuit current is negative—as is J_L for voltages below open circuit.) This assumption relies on the differential equations governing the operation of the cell satisfying the "principle of superposition." This principle states that if a system is linear then its response to several excitations is the sum of the responses to each excitation applied alone. In general the semiconductor device equations are highly nonlinear (with respect to carrier concentrations or, equivalently, quasi-Fermi levels); however, under most commonly encountered circumstances, approximations can be made which render the system linear. The most widely used method of linearization was first introduced by Shockley,[2] where the p-n junction diode is divided into two quasi-neutral regions separated by a depletion region. This, when coupled with domination of diffusion over drift processes in the quasi-neutral regions (i.e., low-injection conditions), and a recombination rate proportional to the excess minority-carrier concentration, leads to linearity in many practical cases.[1,3] The shifting approximation is further discussed in Sec. III A.

Several instances have, however, been discussed in the literature where the principle of superposition (and hence the shifting approximation) has been shown not to hold for solar cells. Probably the most important example is for cells exhibiting a significant series resistance R_s.[1] This affects the boundary condition at the depletion region edge of the quasi-neutral base, making it a function of the current flowing through the device (and hence nonlinear). It is common to correct both illuminated and dark I-V curves for R_s, and in this work we follow the method recently proposed by Aberle, Wenham, and Green[4] whenever it is necessary to correct our data.

Some other proposed causes for departures from superposition are (a) high-injection conditions in the quasi-neutral regions;[1,5] (b) significant depletion-region recombination and generation;[1,5] (c) a voltage dependence of the depletion-region width;[3,6] and (d) interface recombination in heterojunction solar cells.[6] It appears there is no general agreement over the extent to which depletion-region recombination and generation affects the shifting approximation.[3] Also, only the onset of high-injection conditions is considered in this work, so we do not discuss cases (a)–(d) any further here.

In the following section we present one-dimensional (1D) computer simulations which show two additional examples of deviations from the superposition principle in silicon solar cells. In Sec. III we discuss the reasons for this behavior, and in Sec. IV experimental measurements are presented which confirm the predictions of the simulations.

II. SIMULATION PARAMETERS AND RESULTS

A schematic diagram of the basic solar-cell structure investigated in this work is shown in Fig. 1, and its parameters are listed in Table I. Defects, producing energy levels within the forbidden gap, are introduced into this basic structure either (1) at the rear surface, (2) in the p-n junction depletion region, (3) in a thin layer at a variable position in the base, or (4) throughout the bulk of the device. The defect levels are assumed to lie at midgap, but their electron and hole capture rates are varied. A detailed analysis of the dark and illuminated I-V characteristics of such cells has been presented in an earlier article.[7] In the present study we focus on the cases in which a departure from the superposition principle is observed.

[a]Present address: Institut für Solarenergieforschung, D 31860 Emmerthal, Germany.

 0021-8979/94/76(12)/7920/11/$6.00

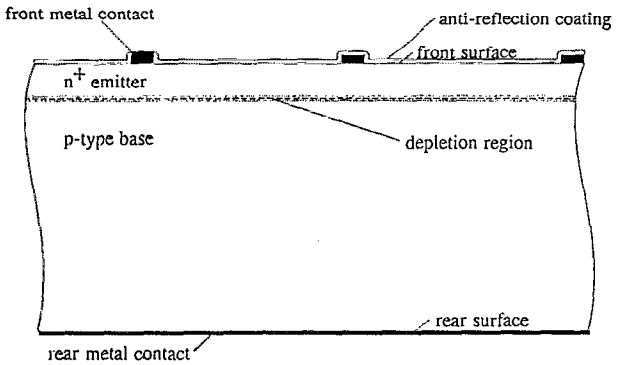

FIG. 1. Schematic diagram of the basic solar-cell structure used in the computer simulations. Defects are introduced into this structure at particular locations to investigate their impact on the I-V curves. The device parameters are listed in Table I.

The cells are modelled using the 1D device simulation program PC-1D (version 3.3).[8] Apart from the radiative recombination constant (which is set to 9.5×10^{-15} cm^3 s^{-1})[9] the default material parameters of PC-1D are assumed. The results under illumination are obtained with an air mass 1.5 global (AM1.5G) spectrum. Complete I-V curves are simulated at various light intensities. In addition, the short-circuit current J_{sc} and open-circuit voltage V_{oc} are determined as functions of light intensity, producing so-called J_{sc}-V_{oc} curves (see, for example, Ref. 7). The J_{sc}-V_{oc} curves are of practical importance since they are first-order approximations to the R_s-corrected illuminated I-V curves (shifted into the first quadrant). As mentioned above, it is known that series resistance produces a departure from the principle of superposition, and hence the J_{sc}-V_{oc} curves are useful in eliminating series resistance effects. It should be noted that only the "intrinsic" series resistance effect due to the bulk resistance is included in our (one-dimensional) simulations, and we do not correct the resulting I-V curves for this R_s; however, for the investigated cell structure, this effect only causes a R_s contribution of 0.028 Ω cm^2, so that its impact on the I-V characteristics of 1 sun cells is negligible (ΔV $<$1.1 mV). Shunt resistance effects and "extrinsic" series resistance effects (from the limited emitter sheet conductivity, the resistance of the front metal grid and the front and rear contact resistances) are not included in these simulations. Although the structures considered here contain allowed states within the band gap, we do not consider subbandgap absorption[10,11] or occupation of these states by photoexcited carriers[12] in this work. The simulations reported are performed for n^+p devices, however, the conclusions are identical for p^+n devices.

Two departures from superposition are observed in the simulations. The first, which we subsequently refer to as departure 1, is a displacement to *smaller* currents of the J_{sc}-shifted illuminated I-V curve relative to the dark curve, at intermediate bias levels. Typical I-V characteristics exhibiting this effect are shown in Fig. 2. The effect is only observed in cells containing defects with unequal electron and hole capture rates (or, equivalently, unequal lifetime or surface recombination velocity parameters). Further, this effect is evident only near the shoulders in the simulated I-V curves which we have shown[7] are due to the *saturation* of Shockley–Read–Hall (SRH) recombination rates[13] via those defects with unequal capture rates. That is, at low forward voltages, the recombination rate is proportional to the excess minority-carrier concentration. As the voltage is increased, a transition occurs and a voltage range is reached over which, even though the minority-carrier concentration increases with voltage, the recombination rate is nearly constant. Departure 1 is most pronounced for cells with uniformly distributed defects [Fig. 2(a)], but is still clearly evident in cells with either a defected rear surface [Fig. 2(b)], or a thin defected layer in the base [Fig. 2(c)]. It is not evident in cells with defects in the depletion region [Fig. 2(d)], at least to the limit of resolution of the simulations. Note that in Fig. 2 the J_{sc}-shifted 1 sun illuminated I-V curves extend beyond V_{oc}, in order to clearly show the whole departure from superposition in each case.

The second departure (departure 2) is observed in all the simulations, to varying degrees, and occurs at small forward-bias voltages. The results obtained for a solar cell with uniformly distributed defects are shown in Fig. 3. These results are also typical of the other three investigated devices. The J_{sc}-shifted illuminated I-V curve is displaced to *higher* currents relative to the dark curve, producing a similar shape to

TABLE I. Simulation parameters of the basic solar-cell structure.

Defects (recombination centers)	None, except those introduced as described in the text. Note: Optical excitation through defect levels is not considered in this work
Base doping	1×10^{16} cm^{-3}, p type (1.4 Ω cm)
Emitter doping	n-type diffusion, surface concentration 3×10^{18} cm^{-3}, Gaussian profile
Junction depth	700 nm
Total cell thickness	200 μm
Front surface recombination velocity	S_{front}=0 cm s^{-1} in the nonmetallized regions
Rear surface recombination velocity	S_{rear}=0 cm s^{-1} in the nonmetallized regions
Temperature	300 K
Reflection: Front surface	Double AR coated with ZnS (560 Å) and MgF_2 (1070 Å), 2.5% contact shading loss
Rear surface	95% reflectance+randomization of reflected light

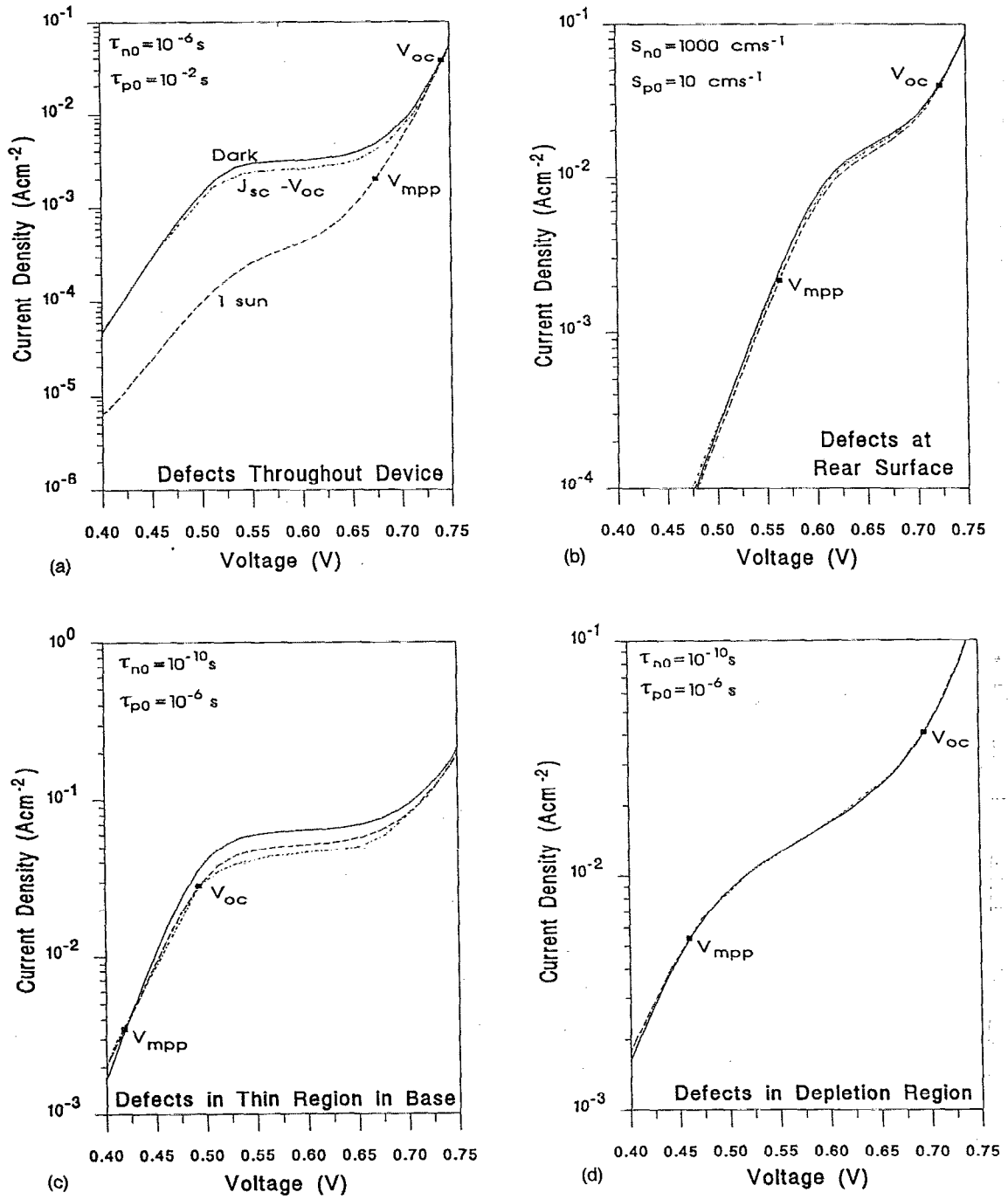

FIG. 2. Calculated dark I-V curve (solid), J_{sc}-shifted 1 sun illuminated I-V curve (dashed), and J_{sc}-V_{oc} curve (dotted-dashed) of the four investigated solar cell structures. In (a) the cell has defects throughout the bulk of the device, in (b) a defected rear surface, in (c) a thin region of defects positioned in the base, and in (d) defects in the depletion region. The electron and hole lifetime or surface recombination velocity parameters of the defects are shown in each graph. Also shown are the open-circuit voltage V_{oc} and MPP voltage V_{MPP} under 1 sun illumination.

one characteristic of a large shunt conductance. The displacement increases with light intensity. It should be noted that the currents of the J_{sc}-shifted curve are the (small) difference between two large numbers, and therefore could be affected by the finite accuracy of the simulation program; however, increasing the convergence tolerance by orders of magnitude did not change the simulated current values, at least to a precision level of 10^{-8} A cm^{-2}. As can be seen in Fig. 3, the J_{sc}-shifted currents of importance for departure 2 are at least two orders of magnitude higher than this limit, and are well behaved functions of voltage, suggesting that the observed effects are not simulation artefacts.

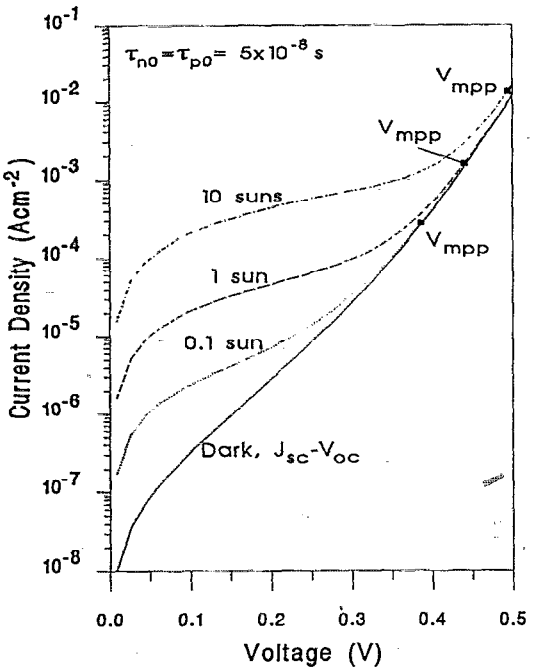

FIG. 3. Typical calculated dark (solid line) and illuminated I-V curves of the investigated solar-cell structures at small forward bias. The dotted line is for 0.1 sun, the dashed line for 1 sun, and the dotted-dashed line for 10 sun illumination. The J_{sc}-V_{oc} curve lies exactly on the dark I-V curve. The curves shown are for a cell with defects throughout the bulk (the lifetime parameters for electrons and holes are shown in the figure). The MPP voltage V_{MPP} is indicated for each light intensity.

III. DISCUSSION

A. Shifting approximation

For a p-n junction solar cell with perfect ohmic contacts (as are assumed here), the current flowing under forward bias in the dark is equal to the total recombination within the device (scaled by the electronic charge q),

$$J_D(V)=qR_D^{\text{tot}}(V)=q\int_{\substack{\text{entire}\\\text{cell}}}R_D^{\text{bulk}}(\mathbf{x},V)d^3x + q\int_{\substack{\text{cell}\\\text{surface}}}R_D^{\text{surf}}(\mathbf{x},V)d^2x, \tag{2}$$

where $R_D^{\text{bulk (surf)}}$ is the bulk (surface) recombination rate in the dark. In contrast, the current flowing in an external circuit under illumination J_L, is directly proportional to the total light-induced generation rate G^{tot} reduced by the voltage-dependent recombination losses within the cell. If the illuminated curve lies in the fourth quadrant (as illustrated in Fig. 4), J_L is given by

$$J_L(V)=q[-G^{\text{tot}}+R_L^{\text{tot}}(V)] =-q\int_{\substack{\text{entire}\\\text{cell}}}G(\mathbf{x})d^3x + q\left(\int_{\substack{\text{entire}\\\text{cell}}}R_L^{\text{bulk}}(\mathbf{x},V)d^3x+\int_{\substack{\text{cell}\\\text{surface}}}R_L^{\text{surf}}(\mathbf{x},V)d^2x\right). \tag{3}$$

The generation rate $G(x)$ is, in general, a weak function of the cell voltage (due to free-carrier and sub-bandgap absorption),[14] however this is neglected in this work. The J_{sc}-shifted illuminated I-V curve (which lies in the first quadrant) is then given by

$$J_L(V)-J_{sc}=q\int_{\substack{\text{entire}\\\text{cell}}}[R_L^{\text{bulk}}(\mathbf{x},V)-R_L^{\text{bulk}}(\mathbf{x},V=0)]d^3x + q\int_{\substack{\text{cell}\\\text{surface}}}[R_L^{\text{surf}}(\mathbf{x},V)-R_L^{\text{surf}}(\mathbf{x},V=0)]d^2x =q[R_L^{\text{tot}}(V)-R_L^{\text{tot}}(V=0)], \tag{4}$$

since $J_{sc}=q[-G^{\text{tot}}+R_L^{\text{tot}}(V=0)]$ (where J_{sc} is negative as shown in Fig. 4).

For the shifting approximation to be valid, the J_{sc}-shifted illuminated and dark curves must very nearly coincide [Eq. (1)], giving

$$R_D^{\text{tot}}(V)=R_L^{\text{tot}}(V)-R_L^{\text{tot}}(V=0). \tag{5}$$

The necessary and sufficient conditions for Eq. (5) to hold *exactly* are linearity with respect to excess carrier concentration of the differential equations governing device operation, their boundary conditions, and the recombination throughout the device.[1] Indeed, this leads to a stricter equality where, for each point $\mathbf{x}$,

$$R_D(\mathbf{x},V)=R_L(\mathbf{x},V)-R_L(\mathbf{x},V=0). \tag{6}$$

However, Eqs. (5) and (6) still hold to a very close approximation in certain special cases, even when the semiconductor equations cannot be linearized in particular regions of the device (such as the depletion region).[1,3,6] This can occur if the photoexcitation has little effect on the carrier concentrations in the nonlinear region, or the net recombination in that region is small compared to that in the remainder of the device.

It is clear from the above discussion that the recombination losses represented by the J_{sc}-shifted illuminated I-V curve do not include the losses at short circuit [see Eq. (4)]. Indeed, this fundamental property of the shifting procedure becomes of crucial importance when recombination in the device saturates, as is evident in Sec. III B. If all recombination losses are to be represented (as is the case in the dark

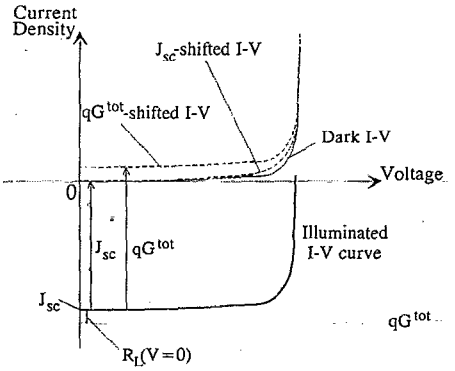

FIG. 4. Schematic diagram showing the standard shifting procedure used for the comparison of illuminated and dark I-V curves. Also shown is the illuminated curve shifted by the light-induced generation rate qG^{tot}. The diagram is not drawn to scale; instead, the differences at low currents are exaggerated for clarity.

I-V curve), then the illuminated curve shifted by qG^{tot} should be plotted (see Fig. 4); however, qG^{tot} is generally unknown, so the J_{sc}-shifted I-V curve is of much greater practical importance.

B. Departure 1

In Appendix A it is shown that the saturation of (SRH) recombination via defects with unequal capture rates (combined with the above-mentioned property of the shifting procedure) is the cause for this effect. Further, the maximum possible separation in current density of the J_{sc}-shifted illuminated and dark I-V curves is determined. This is found to be directly proportional to the integral of the recombination rate at short circuit, over all positions in the device where the recombination is subject to saturation behavior [see Eq. (A4)].

The important conclusion to be drawn from this concerns the *maximum* separation in current density of the measured (or simulated) J_{sc}-shifted illuminated and dark I-V curves. It represents a *lower bound* on the recombination rate at short circuit summed over all regions subject to saturation behavior. Clearly, this gives a direct measure of the minimum reduction in the internal quantum efficiency of the cell due to this mechanism, and hence allows for further device optimization.

In the devices whose I-V curves are shown in Figs. 2(b) and 2(c), only a thin planar section of the device is subject to saturation and the maximum difference in current density reflects the recombination occurring in this layer at short circuit. Recombination in the depletion region is negligible at short circuit, so there is essentially no separation of the curves in Fig. 2(d). When the structure contains uniformly distributed defects, saturation under illumination is reached at different voltages in different regions [Fig. 2(a)], due to the highly nonuniform minority-carrier concentration profiles across the quasi-neutral regions of the device (caused by diffusion of the photogenerated carriers). Despite this, the maximum separation of the dark and J_{sc}-shifted illuminated I-V curves can still be used as a measure of (in this case the total) recombination occurring at short circuit.

If the maximum power point (MPP), for a particular light intensity, lies near the shoulders in the I-V curves then the cell operation under illumination can be markedly different to that expected from the dark I-V characteristics, due to departure 1. This is the case in Fig. 2(a). The position of the shoulders relative to MPP can change for a number of reasons (such as different recombination parameters or light intensities).[7] Thus, although the 1 sun MPPs in Figs. 2(b) and 2(c) are not affected by departure 1, this *need not* be the case for these cell structures. In contrast, the cell with defects only in the depletion region [Fig. 2(d)] would never be significantly affected since there is negligible recombination via these defects at short circuit.

1. J_{sc}-V_{oc} curves

Since the magnitude of the SRH recombination rate at short circuit is a function of light intensity, we see in Fig. 2 that the displacement of the J_{sc}-V_{oc} curve from the dark and illuminated I-V curves at saturation depends on the light intensity at that point. Thus, the J_{sc}-V_{oc} curve may lie above [Figs. 2(a) and (b)] or below [Fig. 2(c)] the J_{sc}-shifted 1 sun illuminated curve.

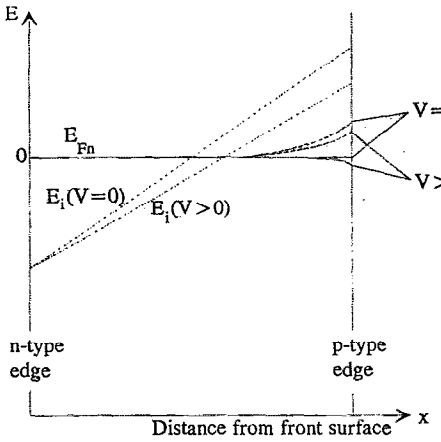

FIG. 5. Schematic diagram of the electron quasi-Fermi level E_{Fn}, across the depletion region of an n-p solar cell for small forward bias (not drawn to scale). The solid lines are for the dark and the dashed lines for the illuminated cell. Also shown is the intrinsic energy level E_i (dotted-dashed line), which is the same under illumination as in the dark for the light intensities considered in this work. Zero energy is fixed at the Fermi energy (at equilibrium) on the n-type edge of the depletion region.

C. Departure 2

This effect is due to the photogenerated current perturbing the carrier concentrations across the depletion region compared to their values in the dark. It is evident only near short circuit because, with increasing voltage, the photoinduced carriers in the depletion region are swamped by forward-injected carriers. The effect shows some similarities to the Kirk effect in bipolar transistors,[15] but the current densities are in general orders of magnitude smaller and there is no movement of the region of high electric field.

Shockley's model of quasi-neutral and depletion regions can be applied to the solar cells investigated in this work. At low forward bias, the SRH recombination rate equation (even for unequal capture rates) is linear in the excess minority-carrier concentration, and the cell operates under low-injection conditions (for the light intensities and doping levels considered). This renders the semiconductor equations linear in the quasi-neutral regions. In addition, the boundary conditions at the front and rear surfaces are also linear.

However, as is shown in Appendix B, the boundary conditions at the edges of the depletion region are not linear, contrary to the commonly made assumption of constant quasi-Fermi levels in the depletion region separated by the voltage across the device.[16] For low injection in the dark[17] and above the maximum power point under illumination,[3] the deviations from constancy of the quasi-Fermi levels across the depletion region have been shown to be negligibly small. This is not the case near short circuit under illumination.[3] More importantly, these changes in the quasi-Fermi levels across the depletion region are a function of the *current* flowing, and hence also of the bias and illumination conditions (Fig. 5).

The result is that the minority-carrier concentrations near the edges of the depletion region are much higher under illumination at short circuit than at zero bias in the dark, in order to maintain the short-circuit current. Furthermore, as the voltage is increased (from $V=0$), the change in minority-carrier electron concentration near the p-type edge of the depletion region under illumination Δn_L is greater than that in the dark Δn_D, by an amount that varies with voltage as [see Eq. (B10)]

$$\Delta n_L - \Delta n_D \approx J_{nL}(V=0)\ Z\left(\frac{1}{\sqrt{\psi_0 - V}} - \frac{1}{\sqrt{\psi_0}}\right), \qquad (7)$$

where Z is a constant which depends on the doping, J_{nL} $(V=0)$ is the short-circuit electron current across the junction (which is assumed independent of position), and ψ_0 is the equilibrium potential difference across the depletion region. An entirely analogous expression holds for holes at the n-type edge of the depletion region.

This behavior of the minority-carrier concentrations is reflected in the quasi-neutral regions and hence also in the recombination throughout the device (due to the linear dependence of recombination on minority-carrier concentration at these bias and illumination levels). As is evident from Eqs. (2) and (4), it is the changes in the recombination rates (from those at $V=0$) that are compared when the J_{sc}-shifted illuminated and dark I-V curves are compared. If the defect density in the solar cell is very low then the effect of the perturbed carrier concentrations on the I-V curves is correspondingly small.

A Taylor-series expansion of the first reciprocal square-root term in Eq. (7) reveals an approximately linear dependence on voltage for $V \ll \psi_0$. This is the reason for the similarity of the J_{sc}-shifted illuminated I-V curve to one affected by a large shunt conductance. Substituting numerical values into Eq. (7), it is found that $\Delta n_L - \Delta n_D$ becomes negligible relative to Δn_D (or Δn_L) above medium bias levels ($\sim$400 mV for the doping levels and light intensities considered here). This is evident in the simulated curves of Fig. 3 as is the dependence on short-circuit current in Eq. (7). Also shown in Fig. 3 is the MPP for each illumination level and in each case it lies well above the voltages at which departure 2 becomes insignificant; however, due to the doping dependence of Z [see Eq. (B10)], it may be possible to choose doping levels such that departure 2 is significant at MPP.

IV. EXPERIMENTAL VERIFICATION

The dark, illuminated, and J_{sc}-V_{oc} current-voltage characteristics of a number of silicon solar cells fabricated at the University of New South Wales (UNSW) have been measured. The apparatus used for this purpose is a computerized I-V tester, capable of measuring both illuminated and dark I-V curves at an accurately determined and highly stabilized temperature. The solar cell sits on a copper block which acts both as a vacuum chuck and rear contact, and the temperature of the block is maintained at 25 °C by a circulating heat transfer fluid from a temperature-controlled bath. Temperature measurement is via a platinum resistance thermometer which was calibrated using a thermocouple referenced to the ice point of water. It should be noted that for the measurements taken in the dark, the temperature of the cell is identical to that of the copper block; however, under illumination the cell temperature rises slightly (about 0.3 °C at 1 sun, for our cells). Such a temperature difference results in a very small shift in voltage (less than 1 mV at 1 sun) of the entire illuminated I-V curve relative to that for the same cell at exactly 25 °C, and is insignificant for this work. The light source consists of four quartz-halogen bulbs (ELH type) connected to a stabilized power supply. A light source that is highly stable over the measurement period is of crucial importance for precise measurement of the illuminated I-V curve near short circuit. It was found that the light intensity of our system was stable to within 0.1% over the time required to scan the I-V curve. High precision in current measurement can be very important near short circuit; however, in our case the precision of the current meter (<0.01%) was at least one order of magnitude better than the limit imposed by the light source.

Two different cell types were fabricated for use in these experiments. The first is a passivated emitter and rear locally diffused (PERL) cell,[18] while the second is a modified passivated emitter and rear cell (PERC).[19,20] Detailed descriptions of these devices can be found in Ref. 18 and 19, respectively; however, the most important cell features for this study are as follows: The PERL cells have been shown to be subject to recombination rate salvation (due to their rear Si-SiO_2 interface).[7,21,22,23] Such cells should exhibit behavior characteristic of the departure 1 case. Owing to resolution limitations imposed by the stability of the light source (0.1%), it is necessary to measure cells which contain a region of high recombination if departure 2 is to be observed. Equally, there should not be a large shunt conductance across the junction, due to the similarity of the resulting I-V curves. A cell with shunting problems is easily detected from its dark I-V curve, and such cells were not used for our measurements. The modified PERC cell's rear contact is made by complete removal of the rear oxide followed by direct evaporation of aluminum onto the entire rear surface and subsequent sintering at 400 °C for 5 min in a nitrogen atmosphere containing 5% hydrogen. This creates a partially shunted Schottky diode as the rear contact which has a very high effective surface recombination velocity ($S_{\text{eff}} \sim 10^6$ cm s^{-1}). Also, the dark I-V curves show no shoulders which suggests the capture rates for electrons and holes at the rear contact are equal.[7] Neither the bulk lifetime nor the p-n junction shunting properties are degraded by the above procedure, resulting in a structure which should clearly exhibit behavior characteristic of departure 2 (and which is free from the effects of departure 1).

Typical results of the measurements are given in Figs. 6 and 7. The theoretically predicted shoulders in the I-V curves of the PERL cells (Fig. 6) are clearly visible. In such real devices it is likely that the defects at the rear Si-SiO_2 interface produce a quasi-continuum of energy levels within the bandgap, leading to the observed smooth transition at "saturation." A distinct downward displacement is evident near the shoulder in Fig. 6(a) in both the J_{sc}-shifted 1 sun I-V curve and the J_{sc}-V_{oc} curves. This becomes even clearer

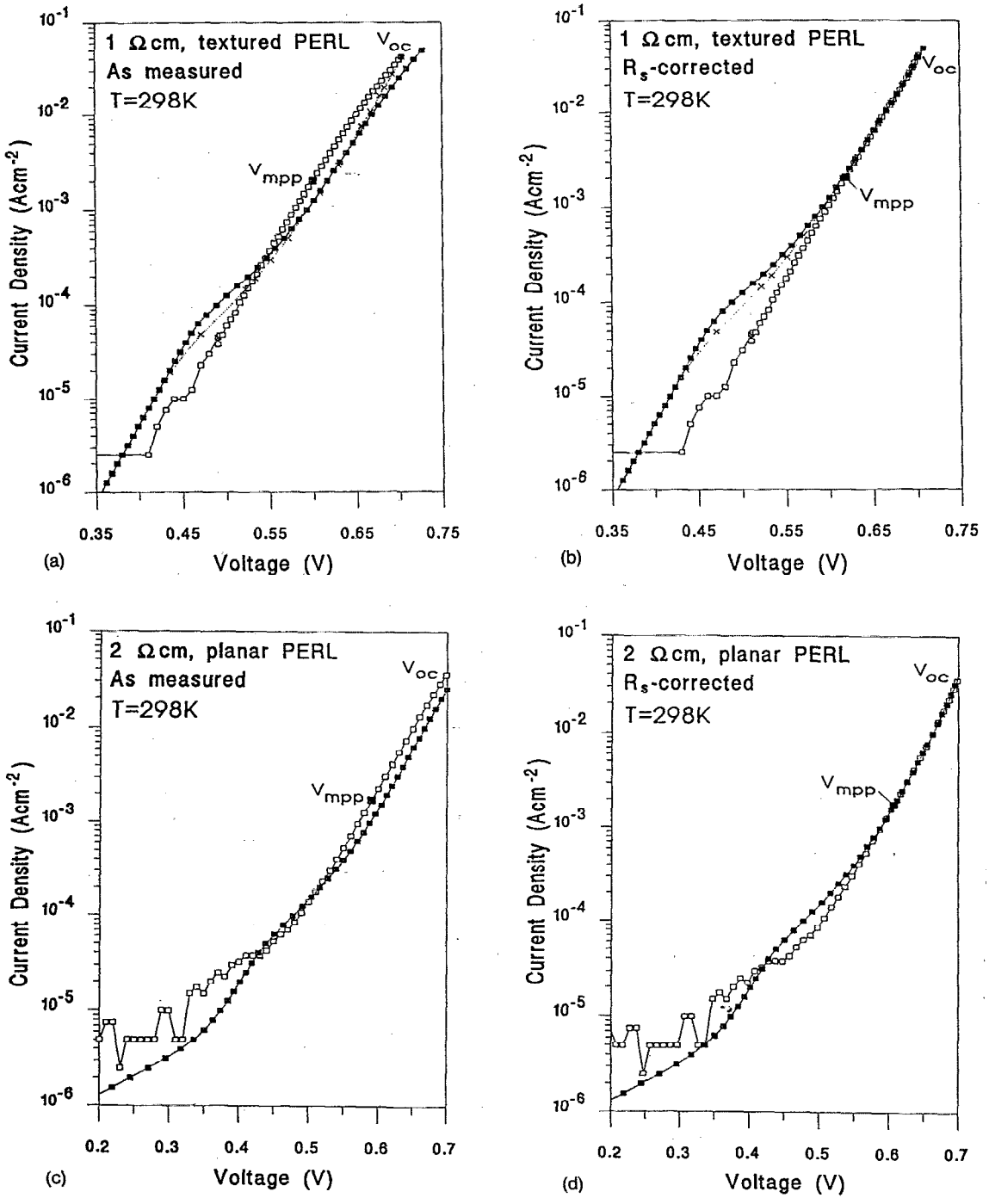

FIG. 6. Measured dark (■) and J_{sc}-shifted 1 sun illuminated (□) I-V characteristics of PERL silicon solar cells. In (a) and (b) the base resistivity is 1 Ω cm and the front surface is textured. In (c) and (d) the base resistivity is 2 Ω cm and the front surface planar. A J_{sc}-V_{oc} curve (×) was also measured for the 1 Ω cm cell. The raw data are shown in (a) and (c), while the R_s-corrected data are shown in (b) and (d). Lines connecting the data points are included as guides for the eye.

when the curves are corrected for series resistance effects [Fig. 6(b)]. The J_{sc}-V_{oc} curve lies above the J_{sc}-shifted 1 sun illuminated curve as expected since the light intensities at the shoulder in the J_{sc}-V_{oc} curve are less than one sun. In Figs. 6(c) and 6(d) both departures are evident, although departure 2 occurs just above the limit of resolution imposed by the light source.

Special care must be taken when correcting the illuminated and dark I-V curves for series resistance effects since, owing to multidimensional effects, the series resistance in the dark $R_{s,\text{dark}}$ is generally significantly smaller than that under illumination $R_{s,\text{light}}$.[4] Using the method recently proposed by Aberle and co-workers,[4] the values of $R_{s,\text{dark}}$ and $R_{s,light}$ used to correct the curves in Fig. 6 are, respectively,

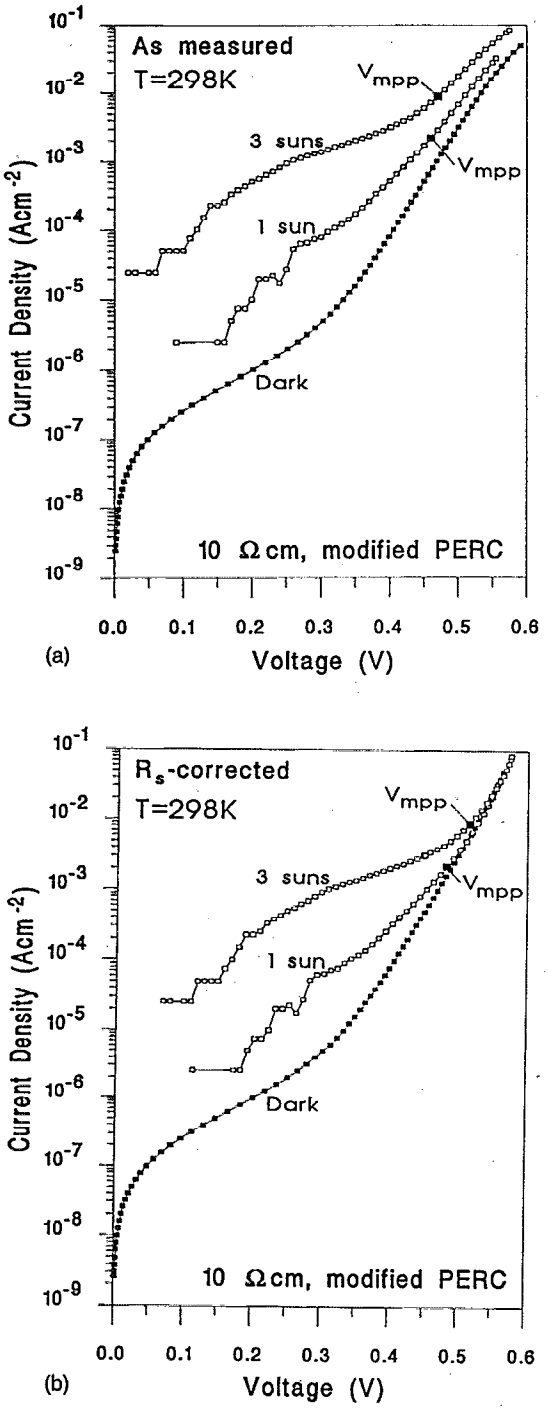

FIG. 7. Measured dark (■) and J_{sc}-shifted illuminated (□) I-V characteristics of a 10 Ω cm modified PERC silicon solar cell. The R_s-corrected data are shown in (b). Lines connecting the data points are included as guides for the eye.

0.38 and 0.48 Ω cm^2 for the textured PERL cell, and 0.42 and 0.50 Ω cm^2 for the planar PERL cell. The value of $R_{s,\text{dark}}$ used for R_s correction in Fig. 7 is 0.55 Ω cm^2 while the values of $R_{s,\text{light}}$ used are 0.72 Ω cm^2 for the 1 sun curve and 0.59 Ω cm^2 for the 3 sun curve. It should be noted that the $R_{s,\text{light}}$ values are subject to uncertainty arising from the injection level dependence of the saturation current (or ideality factor), and any departure from the principle of superposition caused by an effect other than series resistance. For this reason we use a fixed value of $R_{s,\text{light}}$, for each cell, determined near open-circuit conditions (far away from voltages affected by the departures from the superposition principle of interest here).

Comparing Figs. 6 and 2(b), it can be seen that the position, relative to MPP, of the set of shoulders in the measured I-V curves is different to that in the simulated curves. This shift (to smaller currents) of the shoulders in the measured curves is due to fixed positive charge in the rear oxide and the work-function difference between aluminium and p-type silicon.[23] For the PERL cells whose I-V curves are shown in Fig. 6, the saturation behavior is shifted downward such that the MPP is only slightly affected by departure 1. In other PERL cells (for example, with different base doping or oxide charge), departure 1 can be of greater importance at MPP.

Departure 2 is clearly evident in the modified PERC cell of Fig. 7. The dark I-V curve shows that the shunt resistance across the p-n junction is of the order of 10^5 Ω cm^2. Thus, its effect on the I-V curve is small enough that the behavior characteristic of departure 2 is easily distinguished from the ohmic effect. The instability of the light source clearly affects the 1 sun curve below $\sim 10^{-4}$ A cm^{-2}, and the 3 sun curve below $\sim 3\times 10^{-4}$ A cm^{-2}. At lower currents, horizontal line segments are evident which are caused by the limit of resolution of the current meter. In Fig. 7(b), the MPP of the modified PERC cells appear to be slightly affected by departure 2 under both 1 and 3 sun illumination; however, uncertainty in the value of $R_{s,\text{light}}$ used to correct the measured data does not permit a quantitative determination of the impact of departure 2 on the cell's fill factor.

V. CONCLUSION

Two departures from the principle of superposition have been found in 1D computer simulations of standard silicon solar-cell structures with defects positioned at specific locations in the devices. A theory has been proposed to explain these departures in terms of currently accepted models. Furthermore, measurements of silicon solar cells fabricated at the UNSW are presented which clearly exhibit the predicted behavior.

One departure occurs only in cells exhibiting recombination rate saturation and can affect the analysis of the cell's operation at its maximum power point. The improved understanding, provided by this work, of cells that exhibit this behavior (such as the UNSW PERL cells) could lead to future efficiency improvements. The second departure occurs in all solar cells (to varying degrees), and only affects the behavior near short circuit. It is unlikely that this will be important for the performance of silicon solar cells even if optimum doping levels change dramatically in the future; however, these results show that care must be taken when using dark I-V measurements for predictions of solar-cell operation under illumination.

ACKNOWLEDGMENTS

The authors acknowledge contributions of other members of the Centre for Photovoltaic Devices and Systems to this work, in particular J. Zhao and A. Wang who processed the PERL and PERC cells, P. Altermatt for help in taking measurements, and A. Sproul and G. Heiser for useful discussions. S.J.R. gratefully acknowledges the financial support of an Australian Postgraduate Research Award and A.G.A. the support of a Feodor Lynen Fellowship provided by the German Alexander von Humboldt Foundation. This work was supported by the Australian Research Council and the Energy Research and Development Corporation. The Centre for Photovoltaic Devices and Systems is supported by the Australian Research Council's Special Research Centres Scheme and Pacific Power.

APPENDIX A: THE MAGNITUDE AND CAUSE OF DEPARTURE 1

In the following discussion we show how a discontinuity in linearity of the recombination rate (produced by saturation of SRH recombination)[7] leads to a departure from the principle of superposition.

Consider a device in which the recombination rate at a single point $\mathbf{y}$ (or plane in a 1D model), reaches saturation, while at all other points $\mathbf{x}$ the recombination rate remains proportional to the excess minority-carrier concentration and Eq. (6) is valid. Under illumination, saturation may already be reached at short circuit, but in general will be reached at some forward bias voltage $V_L^{\text{sat}}(\mathbf{y})$. Similarly, in the dark the onset of saturation occurs at $V_D^{\text{sat}}(\mathbf{y})$. Note that $V_L^{\text{sat}}(\mathbf{y}) < V_D^{\text{sat}}(\mathbf{y})$ since the carrier concentrations in the dark are always smaller than those under illumination at a given voltage, and hence the onset of saturation occurs earlier under illumination. However,

$$R_L[\mathbf{y}, V_L^{\text{sat}}(\mathbf{y})] = R_D[\mathbf{y}, V_D^{\text{sat}}(\mathbf{y})], \tag{A1}$$

since—as we have shown in our earlier article[7]—the recombination rate at saturation is determined by the majority-carrier concentration (which is essentially equal to the dopant concentration or effective doping at $\mathbf{y}$). Furthermore, since saturation occurs over a range of voltages, one can nearly always find a voltage $V^{\text{sat}}(\mathbf{y})$ for which saturation occurs both in the dark and under illumination,

$$R_L[\mathbf{y}, V^{\text{sat}}(\mathbf{y})] \approx R_D[\mathbf{y}, V^{\text{sat}}(\mathbf{y})]. \tag{A2}$$

Comparing Eqs. (6) and (A2), it is clear that the shifting approximation does not hold at $V^{\text{sat}}(\mathbf{y})$ unless $R_L(\mathbf{y}, V=0)$ is negligibly small.

By taking the difference of Eqs. (2) and (4) at $V^{\text{sat}}(\mathbf{y})$, and using Eq. (A2), one can determine the maximum difference between the dark and J_{sc}-shifted illuminated I-V curves due to recombination at $\mathbf{y}$,

$$(J_D[V^{\text{sat}}(\mathbf{y})] - \{J_L[V^{\text{sat}}(\mathbf{y})] - J_{sc}\})_{\max} = qR_L(\mathbf{y}, V=0). \tag{A3}$$

Thus, if a particular point (or plane in a 1D model) in the cell has reached saturation both in the dark and under illumination, then the dark and J_{sc}-shifted illuminated I-V curves are separated by the recombination rate occurring via this (SRH) mechanism *at short circuit.* Note that if the illuminated curve was shifted by qG^{tot} instead of J_{sc}, then the curves would coincide at $V^{\text{sat}}(\mathbf{y})$ but differ at short circuit (see Fig. 4 and the discussion in Sec. III A).

If more than one point (plane) reaches saturation in the device, the situation becomes more complex since this may occur at different voltages (either under illumination or in the dark), due to the variation in minority-carrier concentrations within the device. If there is a voltage V^s at which all points in the device that can reach saturation have done so, both in the dark and under illumination, then the difference between the J_{sc}-shifted illuminated and dark I-V curves will be

$$J_D(V^s) - [J_L(V^s) - J_{sc}] = q\int_{\mathbf{y}'(\text{bulk})} R_L(\mathbf{y}', V=0)\,d^3x + q\int_{\mathbf{y}'(\text{surface})} R_L(\mathbf{y}', V=0)\,d^2x, \tag{A4}$$

where $\mathbf{y}'$ is the set of all points that can reach saturation. Thus, the right-hand side of Eq. (A4) represents the *maximum possible* difference between the two I-V curves.

APPENDIX B: QUASI-FERMI LEVELS AND CARRIER CONCENTRATIONS ACROSS DEPLETION REGIONS

Quasi-Fermi levels

The following discussion, which assumes a 1D model for current flow in a nondegenerately doped n-p silicon solar cell, is an extension of the approach given by Sah, Noyce, and Shockley[24] and Fahrenbruch and Bube.[25]

Under the assumption that thermodynamic equilibrium is achieved (separately) within the conduction and valence bands of the cell, it can be shown using the semiconductor device equations that the electron current density is given by

$$J_n(x,V) = \mu_n n(x,V)\,\frac{\partial E_{Fn}(x,V)}{\partial x}, \tag{B1}$$

with

$$n(x,V) = n_i \exp\{[E_{Fn}(x,V) - E_i(x,V)]/kT\}, \tag{B2}$$

where x is parallel to the direction of current flow, $E_i(x,V)$ is the intrinsic Fermi-energy level, $E_{Fn}(x,V)$ the electron quasi-Fermi level, n_i the intrinsic carrier concentration, μ_n the electron mobility, T the temperature, and k is Boltzmann's constant. Entirely analogous expressions hold for holes. The relationships (B1) and (B2) lead directly to[25]

$$e^{E_{Fn}(x,V)/kT} = C(V) + \int \frac{J_n(x,V)}{n_i \mu_n kT}\, e^{E_i(x,V)/kT}\,dx. \tag{B3}$$

We now define the zero of energy to be the Fermi energy at equilibrium ($E_{Fn} = E_{Fp} = E_F = 0$), and the zero of position as shown in Fig. 8. Further, in order to simplify the calculations, we assume a linear dependence of E_i on x across the depletion region

$$E_i(x,V) = A_i(V) + B_i(V)x, \tag{B4}$$

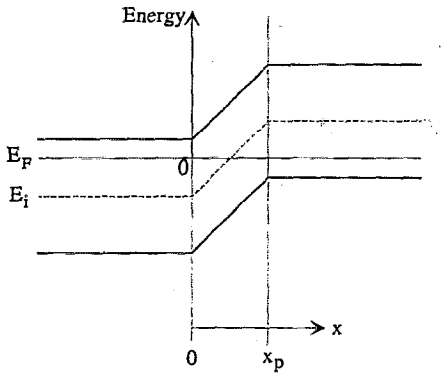

FIG. 8. Schematic diagram showing the assumed band structure for the calculation of quasi-Fermi levels across the p-n junction depletion region.

and an electron current that is constant across the depletion region. These assumptions are approximately satisfied in many practical cases.[16,26] This enables calculation of $C(V)$ in Eq. (B3),

$$C(V)=1-\frac{J_n(V)}{n_i\mu_n B_i(V)}\,e^{A_i(V)/kT} \tag{B5}$$

and

$$E_{Fn}(x,V)=kT\,\ln\left(1+\frac{J_n(V)}{n_i\mu_n B_i(V)}\,(e^{E_i(x,V)/kT}-e^{A_i(V)/kT})\right). \tag{B6}$$

Note that J_n under illumination (which we denote as J_{nL}) is positive under forward bias, while the electron current in the dark (J_{nD}) is negative under forward bias.

Carrier concentrations

We consider the minority carrier concentrations at the p-type edge of the depletion region, but the discussion can be similarly applied to the n-type edge. Under illumination the change in minority-carrier concentration when the voltage is changed from zero to a forward bias V is

$$\Delta n_L=n_i(\exp\{[E_{Fn}^L(x_p,V)-E_i(x_p,V)]/kT\}-\exp\{[E_{Fn}^L(x_p,V=0)-E_i(x_p,V=0)]/kT\}), \tag{B7}$$

where x_p is as defined in Fig. 8. E_{Fn}^L is given by Eq. (B6) under illumination subject to the approximations made in its derivation. Note that E_i is independent of illumination conditions, provided the illumination level is not so high as to cause high-injection conditions. An identical expression to Eq. (B7) is valid in the dark with D replacing L. Substituting Eq. (B6) into Eq. (B7), subtracting the similar expression for the dark, and simplifying gives

$$\Delta n_L-\Delta n_D=\frac{J_{nL}(V=0)(1-e^{-[B_i(V=0)x_p/kT]})}{\mu_n B_i(V=0)}\times\left(\frac{1-e^{-[B_i(V)x_p/kT]}}{1-e^{-[B_i(V=0)x_p/kT]}}\times\frac{[J_{nL}(V)+|J_{nD}(V)|]}{J_{nL}(V=0)}\,\frac{B_i(V=0)}{B_i(V)}-1\right). \tag{B8}$$

This can be further simplified by making the following approximations. First, we determine an expression for B_i under low injection,

$$B_i(V)=\frac{q(\psi_0-V)}{x_p}=\frac{q^{3/2}\sqrt{\psi_0-V}}{\sqrt{2\epsilon[(1/N_A)+(1/N_D)]}}, \tag{B9}$$

where ψ_0 is the potential drop across the depletion region at equilibrium, q the electronic charge, ϵ the permittivity of silicon, and N_A (N_D) is the p- (n-) type dopant concentration. For the bias levels of interest here $B_i>0$, and the exponential terms in Eq. (B8) are much less than unity (for temperatures around 300 K). Second, it is reasonable to assume that any difference between the dark and J_{sc}-shifted illuminated current is very small compared to the short-circuit current, so that the term involving electron currents within the parentheses in Eq. (B8) is essentially equal to unity. These approximations lead to

$$\Delta n_L-\Delta n_D\approx\frac{J_{nL}(V=0)}{q^{3/2}\mu_n}\left[2\epsilon\left(\frac{1}{N_A}+\frac{1}{N_D}\right)\right]^{1/2}\times\left[\frac{1}{\sqrt{\psi_0-V}}-\frac{1}{\sqrt{\psi_0}}\right]. \tag{B10}$$

[1] F. A. Lindholm, J. G. Fossum, and E. L. Burgess, IEEE Trans. Electron Devices **ED-26**, 165 (1979).
[2] W. Shockley, Bell Syst. Tech. J. **28**, 435 (1949).
[3] N. G. Tarr and D. L. Pulfrey, Solid-State Electron. **22**, 265 (1979).
[4] A. G. Aberle, S. R. Wenham, and M. A. Green, in *Proceedings of the 23rd IEEE Photovoltaics Specialists Conference*, Louisville, KY (IEEE, New York, 1993), p. 133.
[5] M. Wolf, Proc. IEEE **51**, 674 (1963).
[6] A. Rothwarf, in *Proceedings of the 13th IEEE Photovoltaic Specialists Conference*, Washington DC (IEEE, New York, 1978), p. 1312.
[7] S. J. Robinson, A. G. Aberle, and M. A. Green, IEEE Trans. Electron Dev. **41**, 1556 (1994).
[8] P. A. Basore, IEEE Trans. Electron Devices **ED-37**, 337 (1990).
[9] H. Schlangenotto, H. Maeder, and W. Gerlach, Phys. Status Solidi A **21**, 357 (1974).
[10] M. Wolf, Proc. IRE **48**, 1246 (1960).
[11] G. Güttler and H. J. Queisser, Energy Convers. **10**, 51 (1970).
[12] M. J. Keevers and M. A. Green, in *Proceedings of the 23rd IEEE Photovoltaics Specialists Conference*, Louisville, KY (IEEE, New York, 1993), p. 140.
[13] W. Shockley and W. T. Read, Jr., Phys. Rev. **87**, 835 (1952); R. N. Hall, *ibid.* **87**, 387 (1952).
[14] M. A. Green, *High Efficiency Silicon Solar Cells* (Trans Tech, Switzerland, 1987).
[15] C. T. Kirk, Jr., IRE Trans. Electron Devices **ED-9**, 164 (1962).
[16] S. M. Sze, *Physics of Semiconductor Devices*, 2nd ed (Wiley, New York, 1981).
[17] A. H. Marshak and K. M. van Vliet, Solid-State Electron. **23**, 1223 (1980).
[18] A. Wang, J. Zhao, and M. A. Green, Appl. Phys. Lett. **57**, 602 (1990).
[19] A. B. Sproul and M. A. Green, J. Appl. Phys. **70**, 846 (1991).
[20] A. W. Blakers, A. Wang, A. M. Milne, J. Zhao, and M. A. Green, Appl. Phys. Lett. **55**, 1363 (1989).

[21] A. G. Aberle, S. Glunz, and W. Warta, J. Appl. Phys. **71**, 4422 (1992).
[22] M. A. Green, S. R. Wenham, J. Zhao, A. Wang, X. Dai, A. Milne, M. Taouk, J. Shi, F. Yun, B. Chan, A. B. Sproul, and A. W. Stephens, Final Report, Sandia Contract No. 66-5863, Sandia National Laboratories, Albuquerque, NM, March 1992.
[23] A. G. Aberle, G. Heiser, and M. A. Green, J. Appl. Phys. **75**, 5391 (1994).
[24] C. T. Sah, R. N. Noyce, and W. Shockley, Proc. IRE **45**, 1228 (1957).
[25] A. L. Fahrenbruch and R. H. Bube, *Fundamentals of Solar Cells—Photovoltaic Solar Energy Conversion* (Academic, New York, 1983).
[26] M. A. Green, *Solar Cells* (Prentice-Hall, Englewood Cliffs, NJ, 1982).